Chapter-5

Discussion

5. Discussion

5.1 Unpromoted model catalysts

The reactivity measurements in connection with pre- and post-reaction characterization on the unpromoted Fe_2O_3 catalyst showed that the clean catalyst initial conversion rate is high and that deactivation is due mainly to reduction of Fe_2O_3 to Fe_3O_4 and to coking. The high initial activity observed is related to the clean Fe_2O_3 surface while the activity of clean Fe_3O_4 is lower. Especially since the addition of oxygen stabilizes the high initial activity, it is important to check if it is the oxygen liberated during substrate reduction (i.e. Fe_2O_3 to Fe_3O_4) which is responsible for the high starting rate on Fe_2O_3. The lattice oxygen could be consumed by the hydrogen produced from the EB dehydrogenation to form water according to the equation (1.3)

$$C_8H_{10} + 3Fe_2O_3 \quad \rightarrow \quad C_8H_8 + 2Fe_3O_4 + H_2O. \qquad (1.3)$$

This would be a simple stoichiometric reaction which could be prevented by admission of O_2

$$2Fe_3O_4 + \tfrac{1}{2}O_2 \quad \rightarrow \quad 3Fe_2O_3. \qquad (1.4)$$

Since our starting films are about 10-20 nm thick and a simple estimation yields the amount of O_2 liberated when the whole film is reduced to Fe_3O_4. Comparison with the amount of St formed (which equals the amount of formed H_2) within the high rate region in Fig. (4.1) (~15 min with rate of 4×10^{15} molecules s^{-1} cm^{-2}) shows that St production is at least by a factor of 700 higher. The dehydrogenation reaction of EB to St over clean Fe_2O_3 is thus essentially catalytic. This means that it could be a unimolecular reaction, where St is produced on the sites where EB dehydrogenates on. i.e. these sites are occupied by EB and St which agrees with what Hirano found [10,11]. The stoichiometric reaction (reduction process (eq.1.3)) may be a side reaction.

The equilibrium thermodynamics of the Fe-O_2-H_2-H_2O system has been investigated experimentally by Muan [61]. Calculations based on thermodynamic data confirm the results [89]. For the reaction temperature of 870 K, Fe_2O_3 is reduced in presence of H_2. Without H_2O, this proceeds to metallic Fe^0 while the presence of H_2O limits reduction to Fe_3O_4. The hydrogen produced during EB dehydrogenation is thus responsible for the observed reduction effects. The role of H_2O is not only to balance coke formation by the coal gasification reaction but also to limit reduction beyond the magnetite (Fe_3O_4) phase [11]

The thermodynamic considerations showed also that hematite (Fe_2O_3) reduction can be prevented by addition of oxygen. The necessary minimum amount corresponds almost to that necessary for the stoichiometric water formation reaction

$$H_2 + \tfrac{1}{2} O_2 \quad \rightarrow \quad H_2O \tag{1.5}$$

The high conversion rate observed with O_2 in the feed Fig. (4.6) corresponds to a conversion of about 10% of the introduced EB. The formed $p(H_2)$ would thus correspond to 10% of $p(\mathrm{EB})$. The necessary oxygen for its oxidation would be 5% of $p(\mathrm{EB})$ and a molar ratio above O_2:EB=0.05 should be sufficient to prevent Fe_2O_3 reduction. If thermodynamic equilibrium would be established, the dashed step curve in Fig. (4.7b) would be expected for the dependence of the steady state rate on the O_2:EB ratio. The measured steady state rates show a reduction with respect to the standard oxygen concentration O_2:EB=0.5 by about 10% for O_2:EB=0.25 and by 25% for O_2:EB=0.15.

There may be two reasons for the rate decay before reaching the theoretical limit of O_2:EB=0.05: Thermodynamic equilibrium may not to be established within the reactor or a part of the oxygen may be consumed for the oxidation of coke. Each EB molecule which is converted into partially dehydrogenated species or graphitic coke and hydrogen, needs 10.5 or 6.5 O_2 molecules for oxidation of all formed products into H_2O and CO_2 or CO, respectively (total oxidation):

$$C_8H_{10} + 10.5\ O_2 \rightarrow 8\ CO_2 + 5\ H_2O \qquad (1.6)$$

$$C_8H_{10} + 6.5\ O_2 \rightarrow 8\ CO + 5\ H_2O \qquad (1.7)$$

In the presented experiments, about 5% of the introduced EB did not show up as aromatics in the GC measurements. This represents the upper limit of EB consumed for coking and a flow ratio O_2:EB=0.525 [reaction (1.6)] or 0.325 [reaction (1.7)]would be necessary to oxidize it continuously. One might think that less oxygen may be necessary since the coke is also partially removed by the water in the feed by the coal gasification reaction. Including the hydrogen formed during dehydrogenation in the coking process, this leads to the sum reaction

$$C_8H_{10} + 16\ H_2O \rightarrow 8\ CO_2 + 21\ H_2 \qquad (1.8)$$

or

$$C_8H_{10} + 8\ H_2O \rightarrow 8\ CO + 13\ H_2. \qquad (1.9)$$

In order to prevent catalyst reduction, it is necessary to oxidize all the produced H_2. The necessary amounts of O_2 correspond to O_2:EB=0.525 and 0.325, respectively, for equations (1.8) and (1.9) and are, of course, the same as without influence of water. It turns thus out that oxidation of coke and of the hydrogen liberated during coking dominate the necessary amount of oxygen to be added. The estimation shows further that the experimentally applied oxygen flow for maximum rate ($EB:O_2=1:0.5$) is near to the optimal level.

The observed reduction of the hematite to magnetite agrees with observations on technical catalysts [12,22,14,86]. However, the high initial rate associated with clean hematite was not observed before. Obviously it was hidden in the start-up and equilibration period, since in most studies found in literature the measurements were done after activating the catalyst under the educts stream for a few hours [10,12,15]. It is therefore likely that only the fully deactivated state was observed in the investigations on technical catalysts. An exception is a recent measurement (Stuttgart experiment) on pressed Fe_2O_3 powder pellets under technical conditions (1 bar, pure EB + H_2O atmosphere, $EB:H_2O=1:6$) Fig. (4.18), where the initial high conversion rate decreased within the first minutes on stream by a factor of ~8-10 [90]. Upon addition of oxygen ($EB:H_2O:O_2=1:6:0.4$), the steady state conversion did not rise to the initial value but could at least be enhanced by a factor of three. The concentration of O_2 was obviously not sufficient for full prevention of reduction and coking. The conversion rate (referred to the BET surface) on the powder catalyst was about two orders of magnitude lower than on the model catalyst which indicates that it is limited by mass and energy transport on the powder catalyst.

In low and medium pressure experiments $p(EB)+p(H_2O) = 3.5\times10^{-6}$ [86] to 0.6 mbar [85] there was clear evidence that defective Fe_2O_3 surfaces are catalytically more active than well ordered ones. In the high pressure experiments presented here, [$p(EB)+p(H_2O) = 36$ mbar], no indications for a defect dependent initial activity was observed but post-reaction analysis showed always that disorder had formed during reaction as seen in the STM image in Fig. (4.2) where the surface is quite rough after reaction and also as deduced from the high background and the diffuse spots in the LEED patterns. Formation of disorder is plausible because of the observed reduction which implies out-diffusion of oxygen and nucleation of magnetite with its different crystal structure. While at low and medium pressures the formation of defects is slow enough so that the influence of initial surface disorder is clearly visible, the more violent reaction conditions at high pressure may accelerate defect formation so that it has happened within the first minutes and may at most influence the first GC data point after gas admission. The importance of defects for the mechanism of the catalytic reaction could thus only be deduced from low pressure experiments.

The final activity after deactivation is definitely not zero. There is strong evidence that it can be ascribed to carbonaceous deposits. It is well known that certain forms of carbon are active catalysts in oxidative dehydrogenation of EB (1.6 chapter 1) which has changed the idea that carbon deposits are always a deactivation source of the catalysts [49,50]. If no oxygen is added and after reduction of the substrate, the only source of oxygen is the water which may supply oxygen according to the dissociation equilibrium at the reaction temperature, a necessary condition for coal gasification. Post-reaction Auger analysis also revealed oxygen at the surface in this case which could indicate that quinoline (C=O) groups on carbon could act as the active sites in the deactivated state, as presented in oxidative dehydrogenation on carbon [51]. When no water is added, even this source of oxygen is lacking. Consequently, no oxygen was visible in AES. However, the final activity in Figs. (4.1, 4.3 and 4.4) was almost the same ~ 0.5×10^{15} molecules s^{-1}

cm^{-2}, independent of the presence or absence of water. The mechanism over the deactivated catalyst is thus not yet clear.

Model catalyst film structure changes under reaction conditions changes and it is not any more like the starting surface. The post reaction characterization and the oxygen on-off experiments Fig. (4.8a and b), show that the surface becomes rougher. This is probably the reason why deactivation after the oxygen is switched off is faster than when starting with the clean Fe_2O_3 without oxygen from the beginning. The roughness results from the re-crystallization caused by dynamic reduction-oxidation process in the film and increases the surface area which improves the solid gas-phase exchange. This may also explain the fast deactivation observed, after switching off the oxygen in the experiments done over the pressed powder pellets in the fixed bed reactor Fig. (4.18). The interesting result in the fixed bed reactor experiment was that the τ_{de} was smaller under reaction in EB and H_2O, without oxygen (normal conditions) but larger after switching the oxygen off after reaction under oxidative condition. This direct drop of the rate after switching the oxygen off could be due to the increase in the roughness or morphology of the catalyst as the results on the model catalyst under the similar conditions showed.

5.2 K-promoted model catalysts

Fig. (4.10). showed clearly that promoting the iron oxide with potassium, lead to a dramatic change in the deactivation behaviour of the catalyst. Also conversion measurements which were run over several model catalysts with different initial potassium content, show that the potassium content have an effect on the initial activity and deactivation rate. Fig. (5.1) summarizes the dependence of the initial conversion rates $\boldsymbol{r}_{in}$ and of the time constant of deactivation t_{de} (assuming an exponential decay of the rates) on the K-content in terms of $\mathbf{I}_K/\mathbf{I}_{Fe}$. Also the initial rates for the unpromoted samples (Fe_2O_3, Fe_3O_4, Fe_2O_3 with O_2 added to the feed) are included. The initial rate decreases and the time constant for deactivation increases with the K-content. A simple explanation of this behaviour would be that K prevents catalyst deactivation by reduction and coking but at the same time reduces or blocks active surface sites. For $\mathbf{I}_K/\mathbf{I}_{Fe}>2.7$, the surface is increasingly covered by $KFeO_2$ [59,73]. The further decrease of the rate in this range suggests that $KFeO_2$ is not the catalytically active phase. However, its presence may be responsible for slow deactivation. The optimal compromise between high rate and slow deactivation may be the composition corresponding to the $K_xFe_{22}O_{34}(0001)$-(2×2) surface.

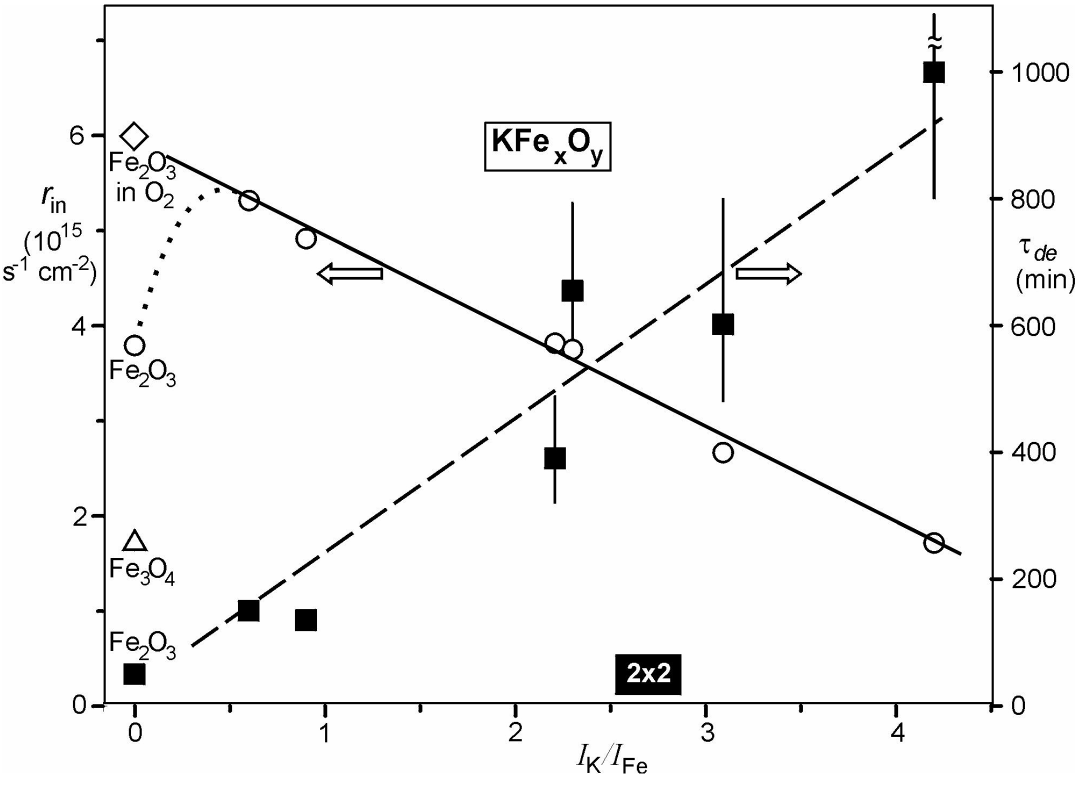

Fig. (5.1). Initial St conversion rate $\mathbf{r}_{in}$ *and time constant for deactivation* $\boldsymbol{\tau}_{de}$ *for samples with different initial K-content in terms of the Auger peak height ratio* $\mathbf{I}_K/\mathbf{I}_{Fe}$*. The composition where the ordered (2X2) structure is formed is indicated.*

For low K-content, the initial rate in Fig. (4.11a) tends towards the rate of Fe_2O_3 with O_2 in the feed while the rate of Fe_2O_3 without O_2 is lower (dotted curve). We believe that this is caused by partial deactivation of Fe_2O_3 before the first data point of the rate curve (Fig. (4.1)) can be taken. It is plausible to assume that the topmost surface layer is partially reduced quite quickly so that the rate approaches that of Fe_3O_4 while addition of O_2 prevents this and preserves the clean unreduced surface.

With oxygen in the feed, the reaction rate on the unpromoted Fig. (4.6) and on the promoted catalyst with low potassium content Fig. (4.14) are very similar concerning both magnitudes and the time dependence. It seems therefore feasible to use oxygen in the feed instead of promotion by potassium; this is confirmed by the weak dependence of the rate over the potassium promoted catalyst on the oxygen amount introduced.

The generally lower coke concentration on potassium promoted catalysts after reaction shows that, the potassium plays a role in catalyzing the removal of carbon deposits In literature [20,21] K_2CO_3 is suggested to be the active sites for the coke gasification.

The gasification of coke goes through a series of sequence reactions which are.

$$K_2CO_{3(l)} + 2\ C_{(g)} \quad \rightarrow \quad 2\ K_{(g)} + 3\ CO_{(g)} \qquad (1.10)$$

$$2\ K_{(g)} + 2\ H_2O_{(g)} \quad \rightarrow \quad 2\ KOH_{(l)} + H_{2(g)} \qquad (1.11)$$

$$2KOH_{(l)} + CO_{(g)} \quad \rightarrow \quad K_2CO_{3(g)} + H_{2(g)} \qquad (1.12)$$

The net equation from these reaction is the removal of carbon:

$$C_{(s)} + H_2O \quad \rightarrow \quad CO_{(g)} + H_{2(g)} \qquad (1.13)$$

The formation of K_2CO_3 during reaction has another effect, which is preventing the fast depletion of potassium mainly as KOH, which has a high partial vapor pressure (~0.1

mbar) at reaction temperature (870 K), since potassium is involved in the cycle of carbon removal explained above. This could explain the moderate loss of potassium observed in our experiments under normal reaction conditions, and the strong loss of potassium under steaming conditions where equation (1.11) becomes the dominant process.

Another function of potassium is to prevent or to retard the reduction of the iron oxide partially by polarizing the Fe-O bond. It was found that in oxide catalysts the electron-donating effect of the alkali metal ions increases the reactivity of the oxygen in the M=O bond (M= transition metal ion in the catalyst) [93].

All results point towards the direction that potassium prevents coking and catalyst reduction but does not directly take part in the catalytic reaction. Since the initial activity on unpromoted Fe_2O_3 and on optimally promoted films ($\mathbf{I}_K/\mathbf{I}_{Fe}$ between 2.2 and 3) is quite similar Fig. (5.1), it is suggestive to assume that the active sites and mechanisms are the same and are related to a stable Fe^{3+}. This is supported by our activation energy value which has been calculated from the reaction experiments at different reaction temperature over both the unpromoted and promoted catalyst (Figs. (4.9, 4.17). The calculations were done by applying Arrhenios equation (1.14)

$$\ln (r) = \ln(A) - E_a/RT \tag{1.14}$$

where r is the rate coefficient, A is a constant, E_a is the activation energy, R is the universal gas constant (8.314 J mol^{-1} K^{-1}) and K is temperature (in degrees Kelvin). Fig. (5.2) shows the plot ln(r) versus I/T(K).. The activation energy was calculated from the linear slope of this plot and found to be ~ 92.1 and 88.7 KJ/mole for the unpromoted and potassium promoted catalyst respectively.

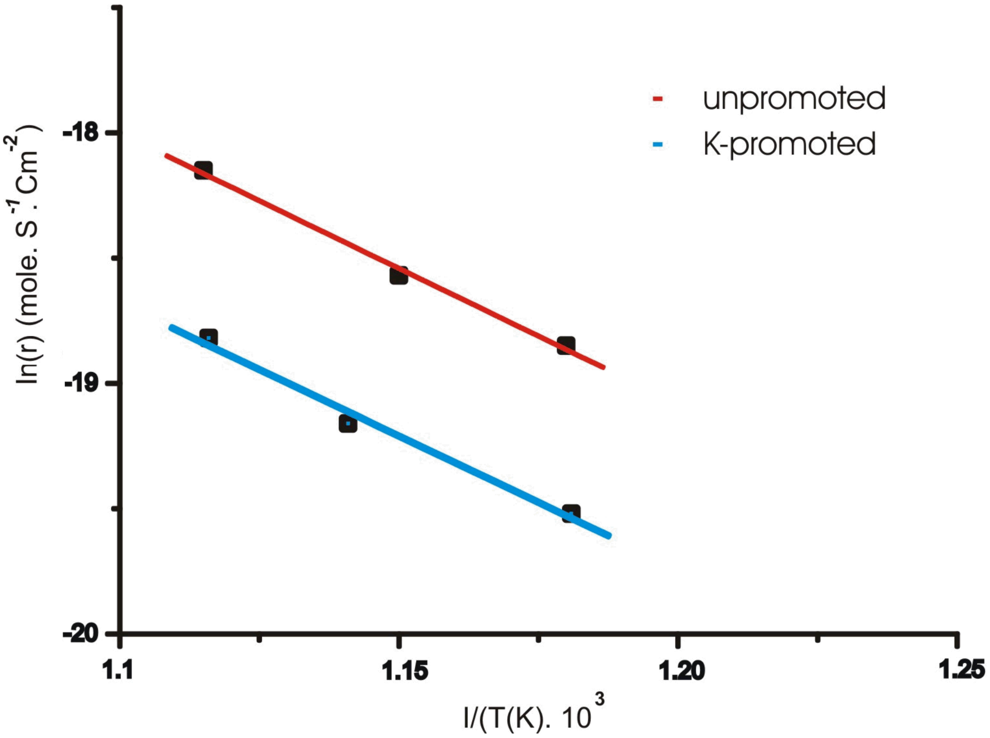

Fig. (5.2). Temperature dependence of the rate of styrene formation over the unpromoted (Fe_2O_3) and potassium promoted iron oxide (KFe_xO_y) model catalysts.

In literature, this was also been claimed to be found for technical and polycrystalline catalysts. The activation energy of the fresh catalyst was found to be lower than the used one [10,12,74]. But, in most cases (according to our knowledge now) the unpromoted catalyst was deactivated and thus not Fe_2O_3 and this could explain the wide range of activation energy (80-140 KJ/mole) found in literature [12,15,22]. Therefore our measurement is the only one which really proves that E_a on both catalysts are equal.

However, in the literature it is always mentioned that the activity of the unpromoted catalyst was an order of magnitude lower than for the promoted catalyst which has directed the development only towards the promoted catalyst. According to the model catalysis results reviewed here, this means that the unpromoted catalyst was most likely deactivated, i.e. reduced and coked [1,2].

Also the addition of oxygen does not change the initial activity dramatically. The mechanism of the main reaction path may therefore not either be influenced by the presence of oxygen. It is not oxidative in the sense that oxygen takes directly part in the catalytic reaction. It rather balances the effects of catalyst reduction by the hydrogen formed in the catalytic reaction and during coking, both being side reactions of the process and it oxidizes the deposited carbon.

The active site requires Fe^{3+} but the Fe^{3+} in Fe_3O_4 is obviously not equally active. It could be that a pure Fe^{3+} environment is necessary as present in Fe_2O_3, $KFeO_2$ and formally also in $K_2Fe_{22}O_{34}$. An alternative explanation was discussed by Kuhrs et al. [88,64] on the basis of the binding energies of EB and St to the different model catalyst surfaces. Due to the existence of iron in the top layer of Fe_3O_4, EB and even more St are bound strongly and may block the surface under reaction conditions while bonding to Fe_2O_3 and $K_xFe_{22}O_{34}$ is much weaker and more similar for EB and St. In hematite, the first layer consists of oxygen, possibly hydroxylated [65] and in K-β”-ferrite, it is most likely formed by K and O [59]. These layers separate the adsorbate from the Fe-layer below but the distance is small enough to let the adsorbate still feel the acidic character of the Fe^{3+} sites underneath. The interaction with Fe_2O_3 and $K_xFe_{22}O_{34}$ is sufficient to bind the EB molecule long enough to the surface to enable dehydrogenation but neither EB nor St so strongly that they block the surface. This is an example for the old wisdom in catalysis that the bonding should be strong enough but not too strong.

Based on the observations that both the right adsorption strength and – at least on unpromoted Fe_2O_3–defects are necessary for high conversion, a model for the catalytic cycle has been proposed [56] and is shown in Fig. (5.2). This model shows the role of defects in the reaction, but in case of reaction in presence of EB and water without oxygen this model works on those parts of surface where are not reduced. Reduction does not occur in each step (4). It occurs in an independent side reaction which slowly decrease the concentration of active Fe_2O_3, but if oxygen is in the feed the reoxidation could happen and the cycle is completed

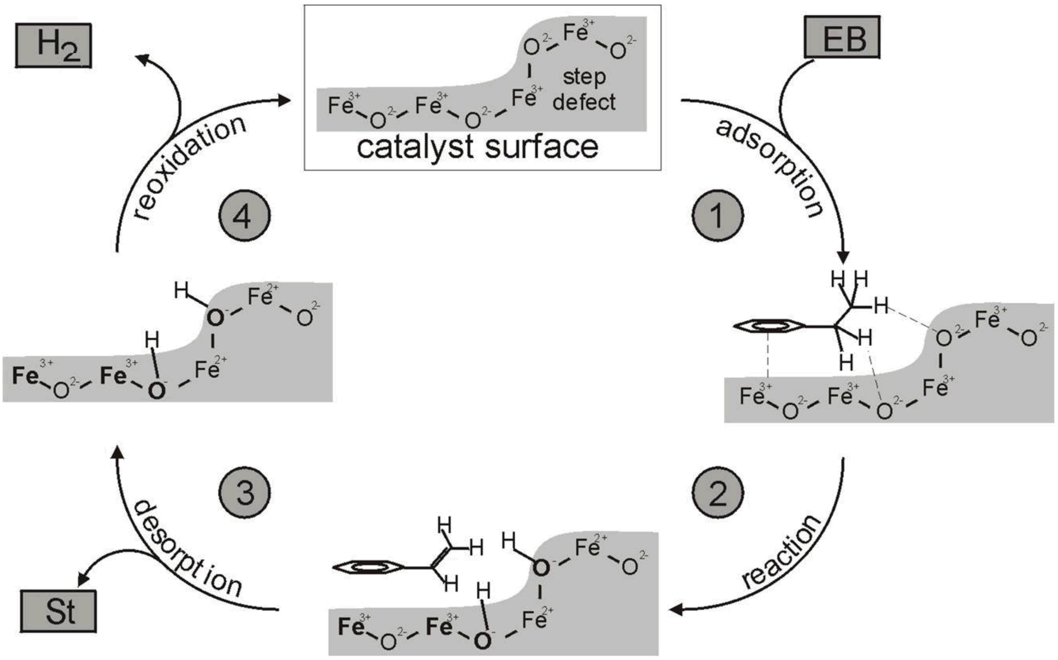

Fig. 5.3. EB dehydrogenation mechanism over the defects sites on the unpromoted (Fe_2O_3) [54]. Step 4 was found not to happen in case of reaction in presence of water alone. The reduction of the Fe2O3 to Fe_3O_4 was found to occur.

The adsorbate-substrate bond via the π-system of the benzene ring is responsible for holding the molecules long enough on the surface. Probably, they are mobile at the reaction temperature and move over the surface until they meet a defect site exposing basic oxygen which attracts the H atoms of the ethyl group and dehydrogenates it. Simultaneously, two Fe^{3+} ions in the vicinity are formally reduced to Fe^{2+} which explains why Fe^{3+} is necessary and why iron with its variable valency is essential. The formed styrene desorbs. The mechanism of H-removal from the catalyst and reoxidation of Fe^{2+} is speculative. However, the presented results show that a direct desorption in form of H_2 is possible. In the main reaction path, it is not removed as H_2O by consuming substrate oxygen which later would have to be replaced by dissociation of water or by reaction with O_2 from the feed (Mars-Van Krevelen mechanism). Substrate oxygen is consumed but this is only a side reaction and leads to reduction of the substrate to Fe_3O_4 which is irreversible when only H_2O and no O_2 is added to the feed [90-92].

So far, nothing is known about the structure of the anticipated protection layer against K-removal on the promoted catalyst which possibly consists of K-carbonate, since the "protection" has to be effective for K only. At the reaction temperature the potassium hydroxide and carbonate mixture is molten, and under the conditions employed of 870 K and a high partial pressure of water vapour, KOH at these conditions is volatile, this was seen on the technical catalyst where the alkali is transported to towards the reactor exit. This loss is inhibited by the partial pressure of CO_2, which increases along the axis of the reactor (due to the gasification of coke). The major part of the alkali in the final section of the reactor is present in the form of relatively involatile potassium carbonate [1,2]. It could be that the local structure of the active sites consists of O above Fe^{3+}, an arrangement similar to that on Fe_2O_3 as proposed by Muhler et. al. Fig. (5.3). Active sites for coke gasification could be surface K carrying a carbonate group, maybe by inclusion of surface O. Earlier results from infrared investigations [94] suggest that free potassium carbonate is not present, but that a complex is formed in which potassium and carbon are linked via an oxygen atom.

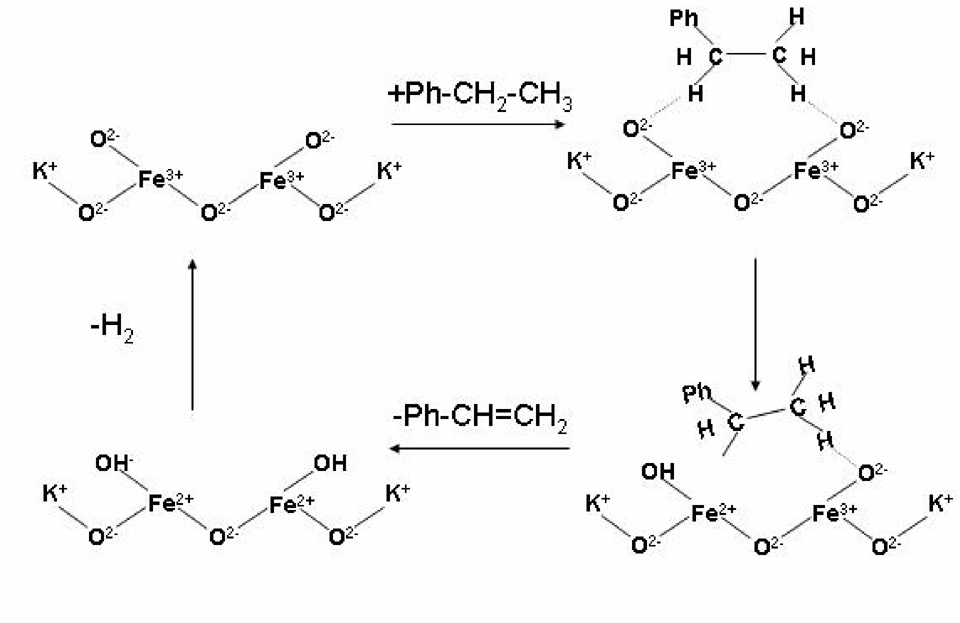

Fig. (5.4) Reaction mechanism proposed by Muhler et. al. [74] for the dehydrogenation of EB to ST over potassium promoted iron oxide catalysts.

Reactivation with water experiment on the promoted catalyst Fig. (4.13a,b) show that reactivation lead to regeneration of the high initial activity by gasification of the of coke deposits. On the other hand it leads to the acceleration of the potassium removal probably as KOH, which has a high vapour pressure at the reaction temperature. This correlates quite well with observations on the technical catalyst, where the results show that potassium at the inlet of the reactor is mainly converted to potassium hydroxide as a consequence of the high partial pressure of steam. This then accelerates the loss and redistribution of the potassium towards the outlet of the reactor or towards the center of the catalyst pellets as a consequence of the endothermicity of the reaction. This leads to a high concentration of the potassium at the outlet of the reactor and the in center of the pellets, and both (center of the pellets and outlet of the reactor) were found to show low or no activity which correlates to what was found on the model catalyst with high potassium contents [2]. The fast removal of the potassium by reactivation on the model catalyst, leads in turn to a faster deactivation of the catalyst by the increase in the carbon deposits. Potassium removal or redistribution is thus the main reason for catalyst deactivation [95].

In the literature, it was proposed that $KFeO_2$ represents the catalytically active surface phase on promoted catalysts while K-β”-ferrite $K_2Fe_{22}O_{34}$ was supposed to be the bulk phase below, representing a K-reservoir for the reestablishment of $KFeO_2$ [7,8]. Previous studies on model catalyst preparation [20,21] indeed showed that $KFeO_2$ forms when a layer of K deposited on Fe_3O_4 is annealed at 700 K. Annealing to the reaction temperature 870 K results in a thin $KFeO_2$ layer or $KFeO_2$ islands on K-β”-ferrite and at 970 K, no $KFeO_2$ is left. The surface is then most likely terminated by a full Fe-O-K layer forming an ordered 2×2 superstructure in LEED. Since surface and bulk composition are in equilibrium at temperatures above about 600 K [59], this surface layer can only be established when the bulk contains an amount of K which corresponds at least to sub-stoichiometric $K_xFe_{22}O_{34}$ ($x \geq 0.67$). The K-promoted films in our study with $2 < \mathbf{I}_K/\mathbf{I}_{Fe} < 2.5$ surely consisted only of K-β”-ferrite without any $KFeO_2$ on the surface. Nevertheless, they deactivate slowly and have a high conversion rate (Figs.(4.10, 4.13a, 5.1)). $KFeO_2$ which forms on the surface for $\mathbf{I}_K/\mathbf{I}_{Fe} > 2.7$ causes the initial rate to decrease further thus ruling out that it is the catalytically active phase. However, the deactivation proceeds even more slowly. It is thus likely that the role of active phase and reservoir phase is inverted, i.e. K-β”-ferrite is the active phase and $KFeO_2$ represents the K reservoir. Intuitively this seems plausible. The coincidence of long-lasting high activity with the presence of the $KFeO_2$ phase does not necessarily mean that it is the active phase. It could be as well that the reservoir phase is necessary to guarantee at least the existence of a sub-stoichiometric of K-β”-ferrite with Fe-O-K- termination while the stoichiometry and the surface K-content drops when the reservoir phase is consumed. The existence of $KFeO_2$ would thus “buffer” the K-β”-ferrite phase against K-depletion by reaction with H_2O.

3- Pressed powder samples

Concerning the deactivation, phase transformation and its prevention by addition of oxygen, the results on the pressed powder samples agree well with the results on the model catalysts. The presented experiments show the validity of the model catalysis approach and the usefulness of surface science techniques in understanding complex catalyst and reaction mechanism. In so far the study represents a successful bridge over the material gap.

The results show that the clean pressed Fe_2O_3 powder catalyst has a high initial activity and it deactivates by reduction to Fe_3O_4 and by coke formation and by degradation of the catalyst as the SEM images, XRD and EDX characterization showed. Admitting some oxygen to the feed can help in maintaining higher conversions and prevents or decreases the rate of deactivation of the catalyst by preventing the reduction and decreasing the amount of carbon deposits. Fig. (5.5) compares the carbon peak on the powder samples after different treatments. The SEM images show that re-crystallization of the particles occurs and which was ascribed to reduction and reoxidation processes.

Quantitatively, the rates of St conversion on the pressed powder catalyst, it becomes clear that the rates on the powder catalyst is considerably lower if referred to its BET surface. Assuming equal rate, the accessible surface area of the powder catalyst is a bout fife times the accessible geometric surface area Due to mass transport limitations. not all pores are accessible. The results show that the catalyst is very active and there is no need to develop it, However an improvement may be expected from engineering and reactor design in order to allow the largest portion of the catalyst surface to be accessible to the reactants.

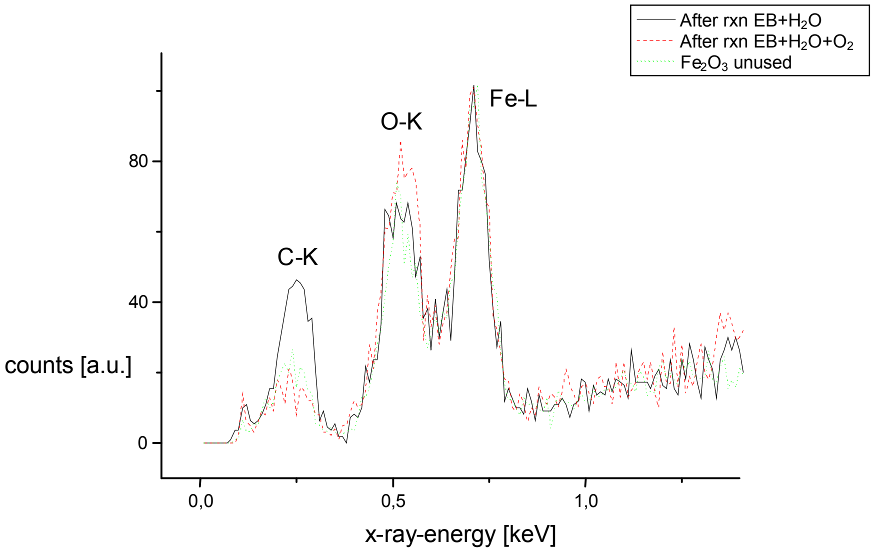

Fig. 5.5. Comparison of the EDX spectra for pressed powder samples after different treatments. The unused fresh pressed powder is also shown for comparison. The spectra are normalized to equal Fe-L intensity.

The low activity of the fresh powder samples shows that the catalyst needs to be activated by cleaning before use in order to obtain a high activity. This may explain why high initial activities have not been observed before on real catalysts.

The SEM images also show that the catalyst morphology changes under the reaction condition, the catalyst brittleness increases. This is in a good agreement with the results on the model catalyst where the roughness of the surface increases under reaction conditions.

5.4 Reaction formalism and catalyst model

5.4.1 Unpromoted iron oxide model catalyst

From the presented results it was concluded that the reaction is catalytic and does not follow a Mars van Krevelen mechanism. It was also clear from the high activity observed that Fe^{+3} ions are essential for high catalytic activity. The deactivation of the unpromoted catalyst occurs by reduction to Fe_3O_4 and by accumulation of carbon deposits, scheme 4 illustrates the reaction mechanism.

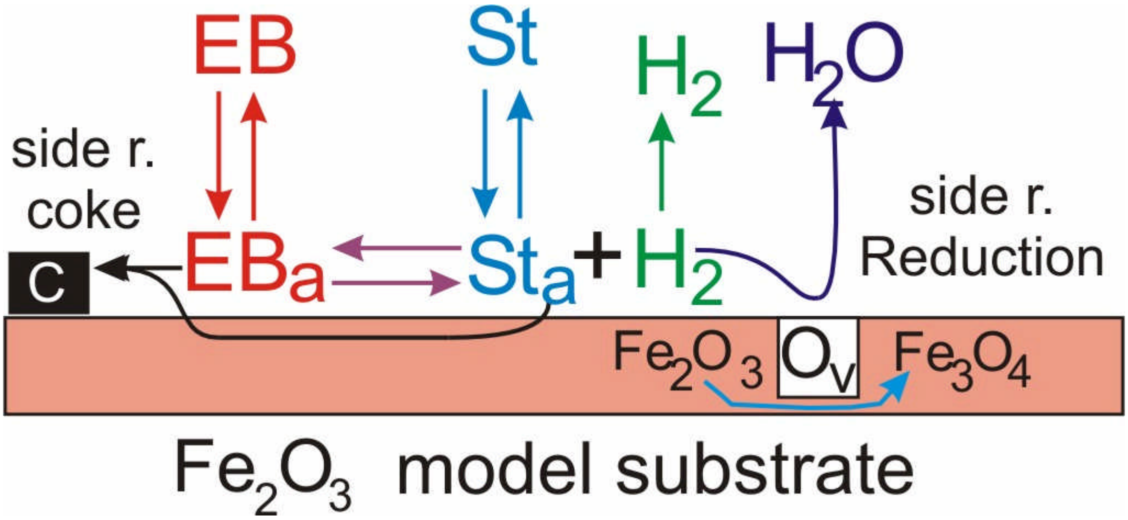

Scheme 4. An illustrative scheme for the main and side reaction pathways of the dehydrogenation of EB over the unpromoted Fe_2O_3 model catalyst.

Water was found not to play a role in the rate determining step. It prevents the complete reduction of the iron oxide to metallic iron and limits reduction to Fe_3O_4. Further it gasifies carbon deposits from the surface by the water gas shift reaction. The role of water is explained in scheme 5.

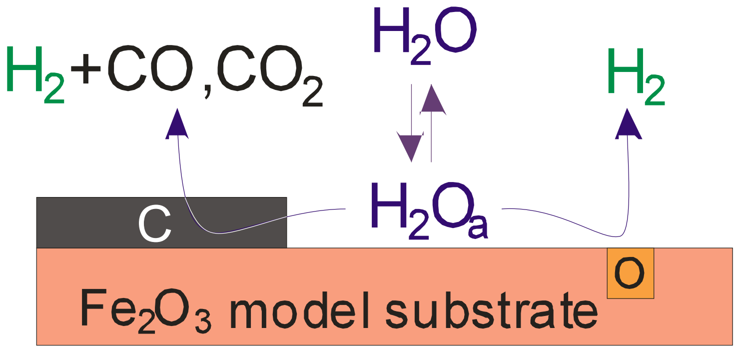

Scheme 5. An illustrative scheme explaining the role of water in preventing the complete reduction of the catalyst and the gasification of carbon deposits

5.4.1 Potassium promoted iron oxide model catalyst.

On the promoted catalyst the main reason for deactivation was found to be the continuous loss or redistribution of potassium from the catalyst. The potassium loss was found to be slower during reaction in the presence of EB than during reactivation with water alone. This could either be due to the presence of some kind of carbonaceous protection layer which seems unlikely or to the formation of a stable phase under the course of reaction like K_2CO_3 which is less volatile than KOH. Less carbon deposits are formed on the promoted catalyst K_2CO_3 is believed to be the active site for the coke gasification. Further, potassium was found also to play a role in preventing the reduction of the iron oxide phase.

The reaction mechanism and side reactions on the potassium promoted catalyst are shown and explained in scheme 6a, and b.

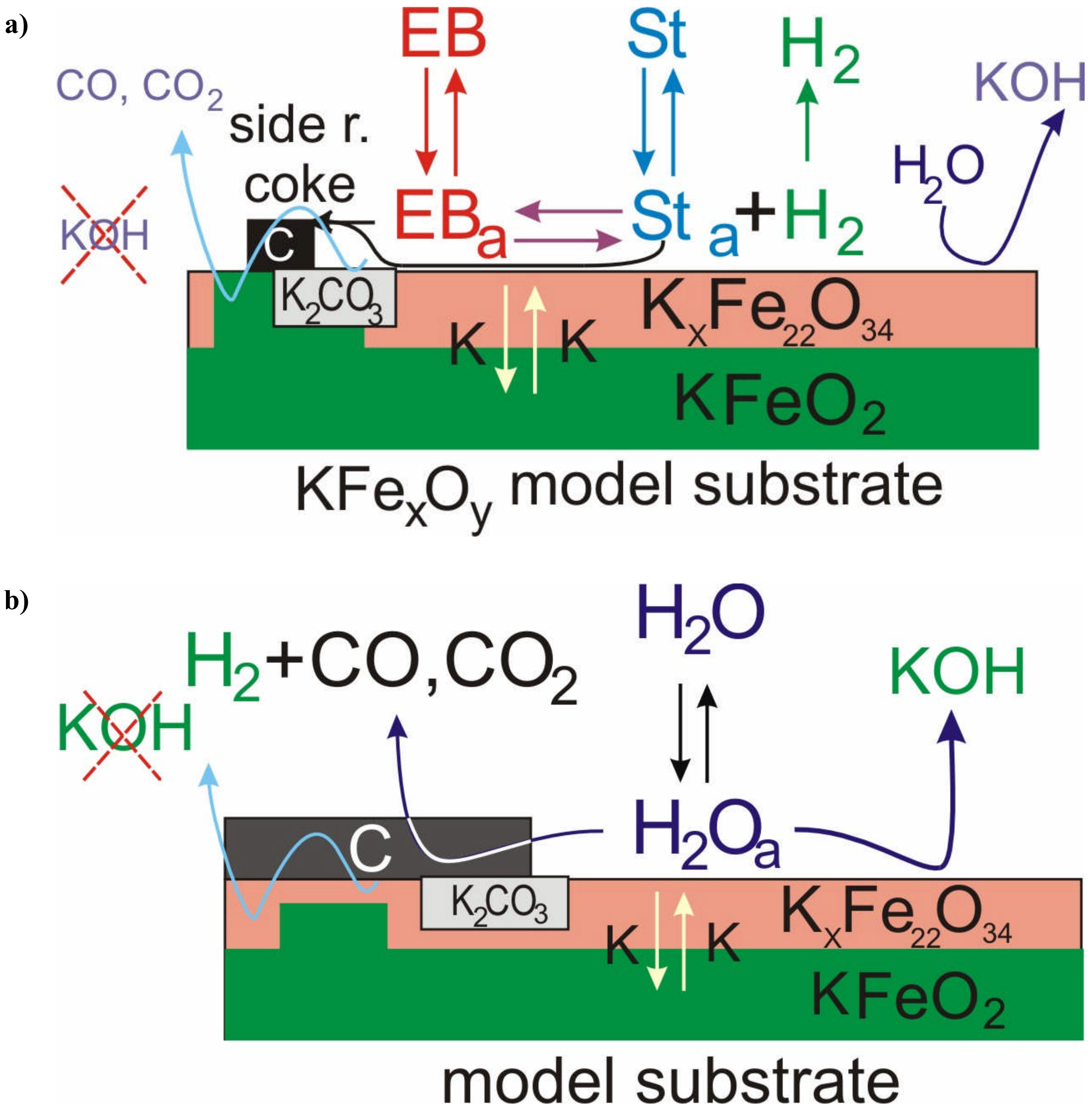

Scheme 6. a) The main and side reaction pathways over the potassium promoted iron oxide model catalyst. b) The role of water in the gasification of carbon deposits and the acceleration of potassium loss.

5.5 Conclusions

The pressure and material gap between reactivity studies in UHV and real catalysis can only be overcome by application of in-situ methods of catalyst characterization and activity measurements under realistic pressure and temperature conditions as has been done in this study. Well defined thin epitaxial films of the compositions $Fe_3O_4(111)$, α-$Fe_2O_3(0001)$and KFe_xO_y were prepared, transferred into a stagnation point micro flow-reactor for conversion measurements and afterwards transferred back for post-reaction surface characterization.

On unpromoted Fe_2O_3, a high initial conversion was observed. Deactivation is caused both by reduction of Fe_2O_3 to Fe_3O_4 and by coking. Water added to the reactant is not involved in the main catalytic reaction. As proposed before, it is essential for gasification of carbon deposits thus limiting its amount. Further it limits reduction of the iron oxide to the oxidation state of Fe_3O_4 and prevents further reduction to metallic iron. The high initial conversion of Fe_2O_3 can be maintained by adding a small amount of oxygen to the feed. This prevents reduction and keeps carbon deposits at a low level. The main dehydrogenation path is a simple catalytic reaction and does not follow a Mars Van-Krevelen mechanism.

Potassium as promotor reduces the build-up of carbon deposits and prevents reduction of the oxide. The initial conversion rate decreases with increasing potassium loading, which is explainable by blocking of active sites by excess potassium. However, high potassium contents lead to slower deactivation by coking. $KFeO_2$ is not the active phase but serves as K-reservoir. Potassium is continuously removed during reaction, most likely in form of volatile KOH. The removal rate is considerably faster if the feed contains only water and no EB. It is suggested that EB, St or their decomposition products react with potassium to form carbonate. “Steaming” the catalyst should thus be avoided. Oxidation in O_2 could be an alternative. Also on the promoted catalyst, it was possible to maintain a high activity by addition of oxygen.

Evidence is given that the existence of Fe^{3+} is not sufficient for high activity. The adsorption strength for EB and St is essential as well. The lower conversion on Fe_3O_4 relates with its higher adsorption strength which may lead to site blocking.

The use of pressed powder sample in the micro-flow reactor was successful and confirmed the results obtained on the model catalysts.